ELSEVIER

Surface Science 363 (1996) 112–120

surface science

# Repulsive interaction of $CO^+$ and a Pt surface derived from very low energy ion scattering

Yoshitada Murata [a,*], Katsuyuki Fukutani [a,b], Hiroshi Nakatsuji [c]

[a] *Institute for Solid State Physics, The University of Tokyo, 7-22-1 Roppongi, Minato-ku, Tokyo 106, Japan*
[b] *Institute of Industrial Science, The University of Tokyo, 7-22-1 Roppongi, Minato-ku, Tokyo 106, Japan*
[c] *Department of Synthetic Chemistry and Biological Chemistry, Faculty of Engineering, Kyoto University, Sakyo-ku, Kyoto 606-01, Japan*

Received 9 September 1995; accepted for publication 27 December 1995

**Abstract**

A high ion-survival probability was observed in ion scattering of $CO^+$ on the Pt(001) surface at very low incident energy ($\leq 100$ eV). This probability is dominated by the repulsive potential in the ion–surface interaction. This repulsive ion–surface interaction is described by two potential energy surfaces. One is the Born–Mayer potential in the long-range interaction appearing at incident energies below 80 eV, and the other is short-range interaction observed in the incident energy range 75–100 eV at an incidence angle of 60°. The latter potential is due to chemical interaction and is predicted by a theoretical work using a $Pt_2$–CO model cluster. This repulsive ion–surface interaction is considered to cause $CO^+$ ion desorption from CO on Pt(111) and neutral desorption from CO on Pt(001), induced by a ns-pulsed ultraviolet laser in the multiphoton process.

*Keywords:* Carbon monoxide; Ion–solid interactions, scattering, channeling; Low energy ion scattering (LEIS); Low index single crystal surfaces; Platinum

## 1. Introduction

We have studied ion–surface interactions on metal surfaces in the incident energy region from a few to 100 eV, i.e. for very low energy ions [1]. Ion scattering work in this energy region induces various dynamic processes, such as activated dissociative adsorption, dissociative scattering, surface trapping and ion sputtering. Reactive scattering of the Eley–Rideal type is the final goal of our study of this system. Another aspect that arises from the scattering of very low energy ions on metal surfaces is the charge exchange between an incident ion and a metal surface. The neutralization of incident and scattered ions is closely related to the electronic structures of the incident ion and the target surface. Akazawa and Murata [2] observed the charge exchange between a Pt(001) surface and $Ar^+$, $N^+$ and $N_2^+$ ions and found that the ion survival probability is high in the very low energy region, decreases with increasing incident energy, and shows a V-shape incident-energy dependence. The ion neutralization process for these systems in the very low energy region is shown to occur through Auger neutralization rather than resonance neutralization [2]. Furthermore, the high survival

* Corresponding author. Present address: Physics Department, Division of Natural Sciences, The University of Electro-Communications, 1-5-1, Chofugaoka, Chofu, Tokyo 182, Japan. Fax: +81 424 84 7403; e-mail: murata@e-one.uec.ac.jp.


*PII* S0039-6028(96)00118-5

probability of incident ions in the very low energy region is due to the penetration depth of incident ions [3].

On the other hand, $CO^+$ ion desorption was induced by a ns-pulsed ultraviolet (UV) laser from CO chemisorbed on Pt(001) [4] and Pt(111) surfaces [5]. This is clearly different from neutral CO desorption. Neutral CO molecules from the Pt(111) surface are desorbed in a single-photon process, while $CO^+$ ion desorption is a three-photon process. The threshold photon energy for $CO^+$ desorption ($\sim$6 eV) is higher than that for CO desorption ($\sim$3 eV) [5]. This result corresponds to the repulsive potential between $CO^+$ and Pt(001) in very low energy ion scattering. The repulsive potential between a $CO^+$ ion and a Pt surface has also been predicted by theoretical study [6], and it is suggested that ion desorption from the Pt surface is caused by direct transition from the ground adsorbate state to the repulsive ionization state.

Ion survival is mainly given by the repulsive interaction between the ion and the surface. Therefore, it is expected that the repulsive potential can be derived from the survival probability in the very low energy region ($\leq$100 eV). The scattering of $CO^+$ from the Pt(001) surface has been observed, and a V-shaped incident-energy dependence was also obtained [7].

## 2. Experimental and theoretical results

### 2.1. Ion scattering

Experimental results on $CO^+$ scattering from Pt(001) have already been published elsewhere [7]. Only an essential part relating to this study is summarized here. $CO^+$ ions were generated from $CO_2$ gas introduced into a Menzinger-type ion source, and mass-selected by an electromagnet installed in an ultra-high vacuum (UHV) chamber. The ion beam was decelerated and focused onto the surface. The scattered ions were detected with a rotatable quadrupole mass filter. The acceptance angle of the entrance aperture of the detector was 4°. The trajectories of transmitted ions through the mass filter were bent through 90° using a deflector before detection with an electron multiplier, and elastically scattered ions were detected.

Fig. 1 shows the incident-energy dependence of the scattered ion yields of $CO^+$ and $N_2^+$ from a Pt(001) surface at an incidence angle of 60° in the specular direction [2,7]. A gradual decrease of the ion yield followed by a steep decrease was observed with increasing incident energy. Further increase of the incident energy shows the V-shaped energy-dependence of the yield. This decrease is described by the transition rate of the charge exchange process, and can be rationalized by assuming that the ion survival probability is dominated by the penetration depth of incident ions into the ion–surface interaction region, rather than the residence time of ions in the vicinity of the surface [3]. The closest distance between the incident ion and the surface is determined by the balance between the repulsive potential in the ion–surface interaction and the normal kinetic energy of incident ions.

Dalidchik et al. [8,9] made a theoretical study of low-energy ion scattering on a metal surface and analyzed our experimental results. They

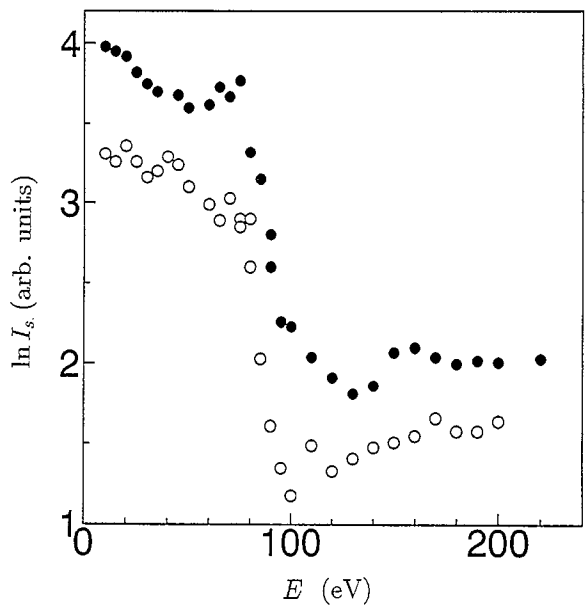


Fig. 1. Logarithmic intensity of the elastically scattered ions as a function of incident energy $E$ for $CO^+$ (○) and $N_2^+$ (●) ions on Pt(001) in the specular reflection. The incidence angle is 60° from the surface normal. The scattered-ion intensity $I_s$ is given in arbitrary units, but a common scale is used for $CO^+$ and $N_2^+$ ions.

pointed out that the scattered ion yields have various structural features, such as a change in slope. In particular, the existence of "h" and "V" peculiarities for the scattered ion yield was noted. The "V"-type minimum is the same as the V-shape described above, while the "h" peculiarity corresponds to the anomalous point observed at ~70 eV in Fig. 1. These structures are interpreted by reionization and de-excitation.

The survival probabilities of $N_2^+$, $N^+$ and $Ar^+$ ions on the Pt(001) surface are nearly identical below 100 eV in the specular direction [2]. From the energy levels of these projectile ions against the Pt valence band, resonance neutralization contributes only for $N^+$ and $N_2^+$ ions. Therefore, the Auger neutralization process in the incoming and outgoing trajectories is dominant, and resonance neutralization is considered to be a minor contribution for projectile ions of $N_2^+$, $N^+$ and $Ar^+$. The observed scattered ion yields show qualitatively good agreement with the theoretical results for the parallel energy dependence of the survival probability due to the Auger neutralization process [10]. As seen in Fig. 1, however, the scattering yield of $CO^+$ is ~1/5 of that of $N_2^+$ in the specular direction. Hence, resonance neutralization might contribute to the charge exchange process in the scattering of $CO^+$ on Pt(001).

The angular distributions of scattered $CO^+$ and $N_2^+$ ions at an incident energy of 30 eV are shown in Fig. 2 [7]. The angular distributions for $N^+$ and $Ar^+$ are similar to that for $N_2^+$. The lobe position for both $CO^+$ and $N_2^+$ scattering is located at ~10° from the surface parallel, but the lobe width for $CO^+$ is narrower than that for $N_2^+$. A similar feature was also observed at other incident energies [7]. This result shows that the normal component of scattered $CO^+$ ions is suppressed and/or converted. If the ion–surface interaction causes inelastic and elastic scattering of incident ions, the normal energy of some ions becomes smaller than the potential barrier, resulting in trapping of the ion in the potential well due to chemical or physical interaction between the ion and the surface. However, elastically scattered $CO^+$ ions in the specular direction are considered to have survived in opposition to Auger neutralization. Therefore, the survival probability can be discussed in terms of the Auger neutralization scheme.

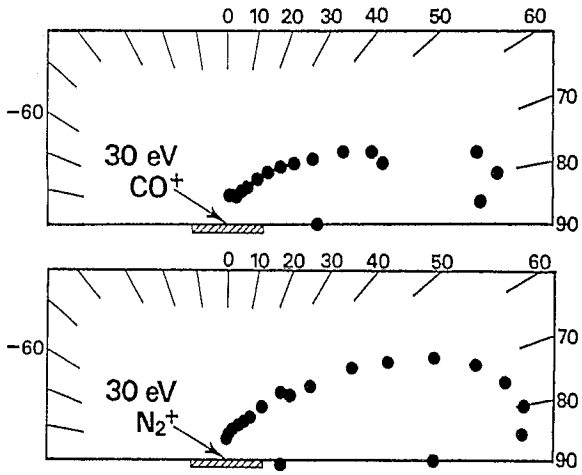


Fig. 2. Angular distributions of scattered ions for $CO^+$ and $N_2^+$ on Pt(001) at an incident energy of 30 eV. The incidence angle is 60° from the surface normal.

### 2.2. Laser-induced ion desorption

Experimental results of the desorption of $CO^+$ from Pt(111) have also been published elsewhere [5]. UV ($\lambda = 193$, 248 and 352 nm) photons generated from an excimer laser (Lambda Physik, pulse duration 11–25 ns) were introduced into a UHV chamber to induce desorption. These photons irradiated the surface at an incidence angle of 25° from the surface normal. The experiment was carried out at 80 K. The desorbed $CO^+$ ions were accelerated to a flight tube facing the sample surface, and were detected by microchannel plates. The desorbed neutral CO was ionized by the (2+1) resonance-enhanced multiphoton ionization (REMPI) method via the $B^1\Sigma^+ \leftarrow X^1\Sigma$ transition. $CO^+$ ions desorbed directly and those ionized by REMPI were detected separately using a flight tube. The cross-sections for CO neutral and $CO^+$ ion desorption have the same value of $(3.5 \pm 1.7) \times 10^{-19}$ cm$^2$ [5]. This value is obtained from decay curves of the desorption intensity from Pt(111) after a CO exposure of 2 L (1 L = $1 \times 10^{-6}$ Torr·s) at $\lambda = 193$ nm, with an incident fluence of 5.6 mJ cm$^{-2}$. Therefore, both CO and

$CO^+$ species are considered to be desorbed from the same adsorption state.

Fig. 3 shows a logarithmic plot of the $CO^+$ and CO desorption yields $I$ versus laser fluence $F$ in laser-induced desorption at $\lambda = 193$ nm. The result definitely reveals the supralinear dependence for $CO^+$ desorption and the linear dependence for CO desorption. The gradient of the logarithmic plot shown by solid lines in Fig. 3 is inferred to be 2.82 and 0.99 for $CO^+$ and CO desorption, respectively. These results suggest that $CO^+$ and CO are desorbed as three-photon and single-photon processes, respectively. The threshold photon energies for $CO^+$ and CO desorption lie between 5.6 and 6.4 eV, and between 2.3 and 3.5 eV, respectively [5].

$CO^+$ desorption is considered to be induced not by substrate excitation but by adsorbate excitation, although neutral CO and NO desorption from Pt surfaces is induced by substrate excitation [11]. Since the three-photon energy of $\sim 6.0$ eV exceeds the ionization potential of gaseous CO (14.1 eV), the direct ionization of adsorbed CO is responsible for $CO^+$ desorption. The supralinear dependence of the desorption yield versus fluence has been reported in NO desorption from a Pd(111) surface [12]. However, this non-linear process can be achieved only by an ultrashort pulsed laser (pulse duration $\leq 1$ ps), due to the high electronic temperature of the substrate out of thermal equilibrium with the phonon bath. Therefore, $CO^+$ desorption from Pt(111) is difficult to reconcile with the mechanism involving substrate excitation in the present experimental condition, in which a ns-pulsed laser was used.

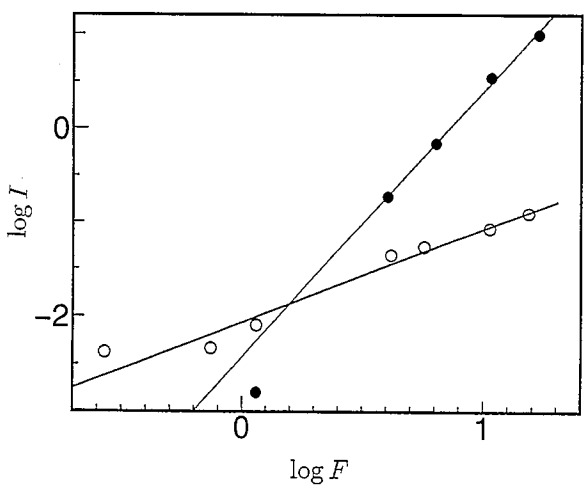


Fig. 3. Logarithmic plot of desorption yields ($I$) versus laser fluence ($F$ in mJ cm$^{-2}$) for desorbed $CO^+$ ions (●) and CO neutrals (○) from CO adsorbed on Pt(111) at 80 K. The induced laser is an ArF excimer laser ($\lambda = 193$ nm, $h\nu = 6.4$ eV, pulse duration 11 ns).

### 2.3. Theoretical calculation of the repulsive potential between $CO^+$ and a Pt surface

Photostimulated desorption of CO and $CO^+$ from a Pt surface, induced by valence electron excitation, was studied theoretically using a $Pt_2$–CO cluster model [6]. Calculations were performed by the single excitation configuration interaction (SECI) and the symmetry adapted cluster (SAC) [13]/SAC-CI [14] methods [15,16]. Almost all the excited states in the non-adiabatic potential energy curves (PECs) having $A_1$, $A_2$, $B_1$ and $B_2$ symmetries due to the excitations from the $\sigma_b$ molecular orbital (MO), are essentially repulsive [6] (the $\sigma_b$ MO is the bonding orbital between the non-bonding (n) orbital of CO and the s orbital of $Pt_2$).

Fig. 4 shows the non-adiabatic PEC of excited states having $B_1$ and $B_2$ symmetries, with the $n$-$1B_1$ and $n$-$2B_2$ states being indicated by open and solid circles, respectively. The n-$1B_1$ state is the lowest ionic state and is attractive, while the n-$2B_2$ state is clearly repulsive. The electronic structures in the separated limit are ionic in $Pt_2^-$ ($s\sigma^*$)–$CO^+$(n) for n-$1B_1$ and $Pt_2^-$*($p\pi$)–$CO^+$(n) for n-$2B_2$. Here, the asterisk on Pt means the excited state, and n-$1B_1$ and n-$2B_2$ denote the first $B_1$ and second $B_2$ states, respectively, having the nature of the excitation from the n orbital of CO. The $CO^+$ ion has a hole in the n orbital (it is therefore denoted $CO^+$(n)) and the electron transferred to $Pt_2$ occupies the 6s and 6p orbitals of Pt, respectively. The n-$2B_2$ state is located 13.9 eV above the ground state at 1.44 Å, which is the equilibrium distance in the ground state. The excitation energy generating the $CO^+$ ion (13.9 eV) is in fairly good agreement with the threshold energy of $\sim 3 \times 6$ eV in $CO^+$ desorption from Pt(111) in the three-photon process.

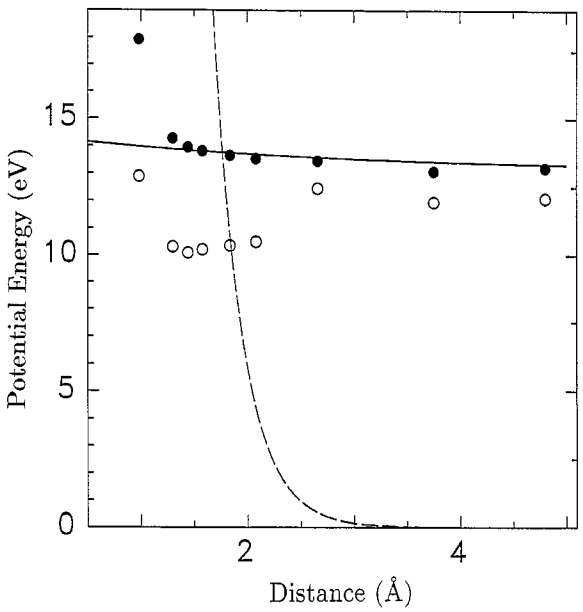


Fig. 4. Non-adiabatic potential energy curve (PEC) of the excited n-$1B_1$ (○) and n-$2B_2$ (●) states on $Pt_2$–CO, calculated using the SAC/SAC-CI method [6]. The origin of the energy is taken at the ground-state minimum. The solid line shows the fitted PEC estimated from the scattered-ion yield of $CO^+$ from Pt(001) and the calculated Born–Mayer potential. The broken line shows the Born–Mayer potential between Pt and C atoms [20].

## 3. Analysis of the ion survival probability

### 3.1. Mechanism of the charge exchange process

The energy dependence of the high survival probability of scattered ions in the very low energy region is analyzed from the derivation of the repulsive interaction between a projectile ion and the surface. The charge transfer process can be explained by a simple analytical model [3,17]. It is assumed that ion neutralization occurs via the Auger-type process. The ion survival probability is given by

$$P=\exp\{-v_c[(1/v_{i\perp})+(1/v_{o\perp})]\}, \quad (1)$$

where $v_{i\perp}$ and $v_{o\perp}$ are the normal velocities of the incoming and outgoing ions, respectively. The survival probability is derived for low-energy ions from the transition rate of Auger neutralization

$$R_t(s)=A\exp(-as), \quad (2)$$

where $s$ is the distance between the ion and the surface. The Auger transition rate of the simple experimental form of Eq. (2) is widely used for the interpretation of experimental results, and is shown by calculation using the optimized variational wave-function for the H(1s)–Au and H(1s)–Al interactions [18]. Here, the characteristic velocity $v_c$ in Eq. (1) is given by

$$v_c=(A/a)\exp(-as_0), \quad (3)$$

where $s_0$ is the ion–surface distance at the turning point. If the characteristic velocity is constant, the Hagstrum relation [19] is satisfied. This situation appears in the incident energy region above 100 eV in Fig. 1, i.e. the survival probability decreases with decreasing incident energy.

If the ion–surface interaction potential is given by a Born–Mayer type repulsive potential [20]

$$V(s)=B\exp(-bs), \quad (4)$$

energy conservation gives us a relation of

$$mv^2/2=mv_\parallel^2/2+B\exp(-bs_0), \quad (5)$$

at the closest distance $s_0$ in the specular reflection for elastically scattered ions. Since the parallel component of ion velocity $v_\parallel$ is conserved for the specular reflection, Eq. (5) is represented by

$$B\exp(-bs_0)=E_\perp, \quad (6)$$

where $E_\perp=mv_\perp^2/2$ is the normal incident energy. Then,

$$s_0=-(1/b)\ln(E_\perp/B). \quad (7)$$

Substituting Eq. (7) into Eq. (3), the characteristic velocity is

$$v_c=(A/a)(E_\perp/B)^{a/b}. \quad (8)$$

Since parameters $a$ and $b$ are derived from overlapping of the same wave-function, the relation $a\approx b$ is considered to be satisfied. Then,

$$v_c=AE_\perp/aB, \quad (9)$$

that is, the characteristic velocity is not constant but depends on the normal energy of the incident ions. Substituting Eq. (9) into Eq. (1), the scattered ion yield $I_s$, which is proportional to the survival

probability $P$, is given by

$$I_s = KP = K \exp(-A\sqrt{2mE_\perp}/aB), \quad (10)$$

for elastic scattering in the specular reflection. A linear relation for $\ln I_s$ versus $\sqrt{E_\perp}$ will be obtained if the relation $a \approx b$ is satisfied. Fig. 5 shows the scattered ion yield for $CO^+$ shown in Fig. 1 replotted as a function of $\sqrt{E_\perp}$. The curve can be fitted by two straight lines, as shown by broken lines in Fig. 5. This result shows that the relation $a \approx b$ is satisfied, and the ion–surface interaction is represented by two different repulsive potentials.

The gradient $\alpha$ in Fig. 5 gives us useful information on the exponent of the repulsive potential, i.e. $\alpha = A\sqrt{2m/aB} \approx A\sqrt{2m/bB}$. Figs. 6a and 6b show the scattered ion yields for $N_2^+$, $Ar^+$, $Ne^+$ and $O_2^+$, as well as $CO^+$, observed in the specular reflection at an incidence angle of 60° [2,7] in the form $\ln I_s$ versus $\sqrt{E_\perp}$. At perpendicular energies below ~16 eV, the gradients for these ions have a common value. This result means that the interaction potential in this region does not reflect chemical properties. That is, the interaction at a long distance from the surface can be described by the Born–Mayer type potential of Eq. (4). On the other hand, the steep gradient in the intermediate energy region appears clearly only for $CO^+$ and $N_2^+$. The intermediate energy region is considered to be described by the chemical interaction predicted by the theoretical study. This region is

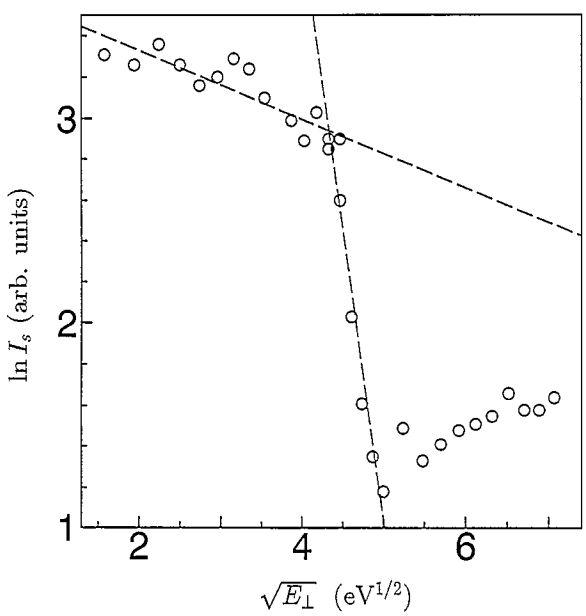


Fig. 5. Scattered-ion yield $I_s$ of $CO^+$ from Pt(001) for the $\ln I_s$ versus $\sqrt{E_\perp}$ curve replotted from the curve of Fig. 1. The broken lines are fitted lines.

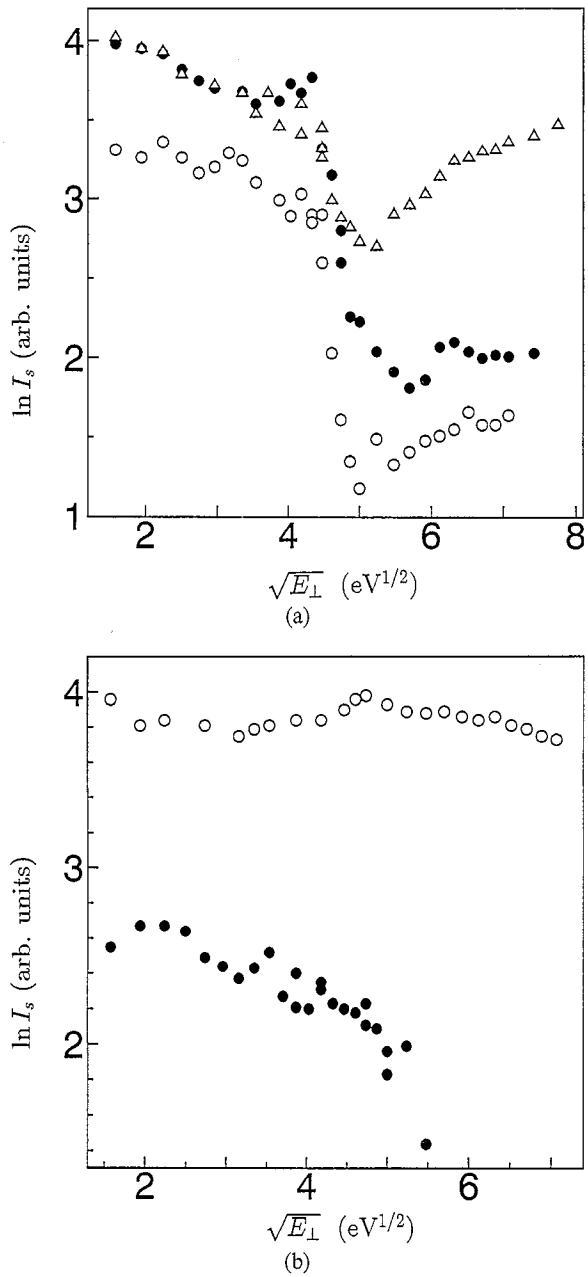


Fig. 6. Scattered-ion yields in the $\ln I_s$ versus $\sqrt{E_\perp}$ curve of (a) $CO^+$ (○), $N_2^+$ (●) and $Ar^+$ (△); (b) $Ne^+$ (○) and $O_2^+$ (●) from Pt(001). The intensity scale is common to all of these ions.

narrow for $Ar^+$ and does not appear for $Ne^+$ and $O_2^+$. The chemical interaction between a projectile ion and the Pt surface for $CO^+$ and $N_2^+$ is considered to be similar. For a projectile ion of $Ar^+$, a weak repulsive interaction appears in the intermediate energy region due to the large polarizability of the Ar atom, although no chemical interaction exists. On the other hand, no chemical interaction exists for $Ne^+$, and the chemical interaction is too strong for $O_2^+$ to have a repulsive interaction.

### 3.2. Estimation of the repulsive potential

The intermediate energy region is related to the chemical interaction predicted by theoretical calculation of the repulsive potential of $CO^+$ desorption. This interaction is clearly observed in $CO^+$ and $N_2^+$ scattering on the Pt surface. In this subsection, we estimate the exponent of the repulsive potential due to chemical interaction from the scattered ion yield. The interaction potential has a smaller exponent at the closer ion–surface distance, as inferred from Fig. 5, and an excitation energy in addition to the Born–Mayer type interaction is necessary. Therefore, the repulsive interaction potential in this region is modified as

$$V(s) = B\exp(-bs) + C, \tag{4'}$$

where $C$ is the excitation energy to an ionized state (i.e. it is considered to be the excitation energy of the n-$2B_2$ state shown in Fig. 4). Using Eq. (4'), Eq. (7) is replaced by

$$s_0 = -(1/b)\ln[(E_\perp - C)/B]. \tag{7'}$$

If the relation $a \approx b$ is also satisfied, the characteristic velocity is given by

$$v_c = A(E_\perp - C)/aB. \tag{9'}$$

Since the modification of Eq. (4) to Eq. (4') is simple, the relation $a \approx b$ is also considered to be satisfied.

Substituting Eq. (9') into Eq. (1), the scattered ion yield $I_s$ in the specular direction is given by the relation

$$\sqrt{E_\perp}\,\ln(I_s/K) = -(A\sqrt{2m}/aB)(E_\perp - C), \tag{11}$$

where the proportional constant $K$ is a common value in low and intermediate energy regions and is obtained from Fig. 5 ($\ln K = 3.665$). A linear relation for $\sqrt{E_\perp}\ln(I_s/K)$ versus $E_\perp$ is expected to be satisfied, and the gradient has the same form as that in the $\ln(I_s/K)$ versus $\sqrt{E_\perp}$ curve, i.e. $\alpha \approx A\sqrt{2m}/bB$. A linear relation was also obtained for the $\sqrt{E_\perp}\ln(I_s/K)$ versus $E_\perp$ curve in the intermediate energy region, as shown by the solid line in Fig. 7. The gradient $\alpha$ is 1.590, and the excitation energy $C$ is 16.9 eV.

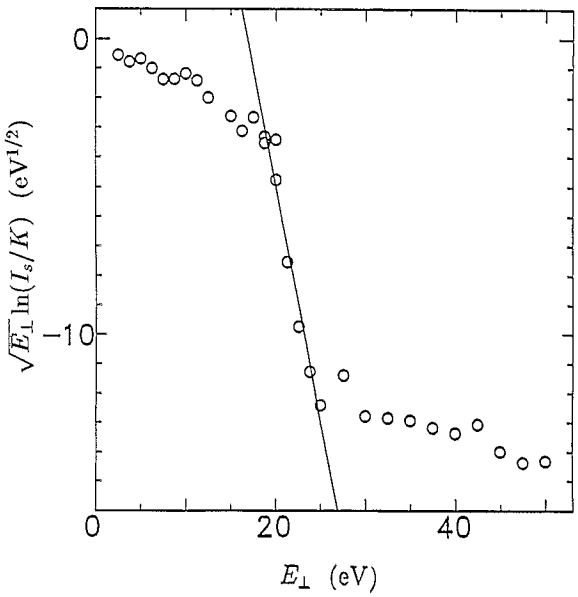


Fig. 7. Scattered-ion yield in the $\sqrt{E_\perp}\ln(I_s/K)$ versus $E_\perp$ curve of $CO^+$ from Pt(001) replotted from the curve of Fig. 1, where the parameter $K$ obtained from Fig. 5 is used. The solid line shows the fitted line in the intermediate-energy region.

The exponent of the repulsive potential estimated from the observed gradient can be compared with the theoretical potential of the n-$2B_2$ state shown in Fig. 4. The observed gradients $\alpha \approx A\sqrt{2m}/bB$ obtained from the $\ln I_s$ versus $\sqrt{E_\perp}$ curve in the low-energy region (Fig. 5) and from the $\sqrt{E_\perp}\ln(I_s/K)$ versus $E_\perp$ curve in the intermediate-energy region (Fig. 7) are $\alpha_l = 0.167$ and $\alpha_i = 1.59$, respectively. On the other hand, the exponent $b_{BM}$ of the Born–Mayer potential for Pt–C is calculated to be 3.65 $Å^{-1}$ from a table given by Abrahamson [20]. If it is assumed that the ratios of pre-exponential factors $A/B$ contained in both $\alpha$s have

the same value, the exponent $b$ in the chemical interaction potential can be estimated from the relation $b = b_{BM}\alpha_1/\alpha_i$, and $b = 0.38\ \text{Å}^{-1}$. The assumption of $A/B$ having the same value is considered to be acceptable, since the interaction potential has the same exponential form in the projectile–surface distance $s$. The curve fitted to the repulsive potential of the n-$2B_2$ state using $b = 0.38\ \text{Å}^{-1}$ is shown by the solid line in Fig. 4, although the excitation energy $C$ is changed as a fitting parameter. The broken line in Fig. 4 shows the Born–Mayer potential between Pt and C atoms [20]. Although the ground state in ion scattering might be given by the n-$1B_1$ state, the Born–Mayer potential should be considered to be that of the ground state in the interaction between Pt and CO.

## 4. Discussion

A fairly good agreement is obtained between the theoretical repulsive potential and the potential estimated from the ion scattering with the aid of the calculated exponent in the Born–Mayer potential, as shown in Fig. 4. However, this estimated value for the exponent is slightly smaller than the calculated exponent for the n-$2B_2$ state. Furthermore, the exponent $b$ was derived using a rough approximation which disregards the orientational effect for the incident molecule. This result suggests that $CO^+$ ion desorption from Pt(111) induced by an ns-pulsed laser is caused by the repulsive potential between $CO^+$ and the Pt surface via the direct excitation process from the ground state to the ionized adsorbate state. The excitation energy in laser-induced ion desorption (estimated from the threshold photon energy) is $\sim 18$ eV, because of three-photon process. This value is in good agreement with the excitation energy estimated in the present study, $C = 16.9$ eV. The value of 16.9 eV corresponds approximately to the perpendicular energy where the sudden reduction in the scattered ion yield occurs.

$CO^+$ and CO desorption from Pt(001) were also found to occur as two-photon and three-photon processes, respectively, at 193 nm [4]. The three-photon process of neutral CO desorption is considered to occur after reneutralization. In contrast to $CO^+$ desorption from Pt(111), active species for the CO desorption from Pt(001) are considered to be adsorbed at the step site induced by the adsorption-induced restructuring from a hexagonal to a $(1 \times 1)$ surface, in analogy to NO desorption from Pt(001) [21,22]. In the step site of the substrate, the electron density is so high that the desorbed $CO^+$ ions are rapidly neutralized on the surface. Thus, the same three-photon process of both $CO^+$ desorption from Pt(111) and CO desorption from Pt(001) is considered to be responsible for ion desorption due to the repulsive interaction between ion and surface.

It is remarkable that $CO^+$ desorption from Pt(001) requires the absorption of only two photons, compared with three photons for CO desorption from Pt(001) and for $CO^+$ desorption from Pt(111). Since direct ionization requires more energy, the initial step of the $CO^+$ desorption process must be valence electron excitation in adsorbed CO, and ionization will follow as a result of excited electron transfer to the substrate, as proposed by Burns et al. for NO and CO ESD from Pt(111) [23]. $CO^+$ desorption can proceed from this ion resonance before reneutralization.

We now compare the estimated quenching rate of the ion in ion scattering with that of the desorbed particle in laser-induced ion desorption. First, we consider laser-induced desorption. The observed intensity of desorbed $CO^+$ ions has a similar value to that of desorbed neutrals obtained from the REMPI signal, as seen in Fig. 3. The detection efficiency in the $(2+1)$ REMPI of CO is $\leq 10^{-3}$, which is estimated from the ionization cross-section in the $(2+1)$ REMPI process and the limited range within the energy and angular distributions of desorbed neutrals. On the other hand, the detection efficiency of $CO^+$ ions is nearly unity. Thus, the relative number of the desorbed ions to the desorbed neutrals in laser-induced desorption is $\sim 10^{-3}$.

Next, we estimate the relative number of surviving ions to scattered neutrals in $CO^+$ ion scattering from Pt(001). This value is roughly estimated from the incident beam current and the scattered ion intensity, and is $\sim 10^{-3}$ at an incident energy of 10 eV in the specular direction. Thus, the relative number is $\sim 10^{-4}$ at 80 eV, as estimated from Fig. 1. This estimation is performed from data observed in the specular direction. In the angular

distribution of scattered $CO^+$ ions from Pt(001) at 30 eV, the lobe position for $CO^+$ is located $\sim 10°$ from the surface parallel at an incidence angle of 60° from the surface normal, as shown in Fig. 2. Furthermore, the lobe widths at incident energies of 70 and 100 eV are narrower than that at 30 eV [7]. Thus, the scattered intensity integrated over the whole scattering angle is ten times higher than this value, and the estimated quenching rate of the ion in the scattering experiment is of the same order of magnitude as the desorbed ions in the laser-induced desorption experiment. However, the transition probability to the ionized state due to the three-photon process is assumed to be the same as that to the excited state due to the single-photon process.

An alternative explanation of the sudden reduction in the scattered ion yield was offered by Kovalevskii et al. [24]. The sharp decrease in ion survival probability is caused by level crossing between the electronically excited state and the ion state. The sharp decrease occurs due to resonance neutralization to the ground state.

Another type of sudden reduction was observed in the inelastically scattered ion yield of $N_2^+$ from Al(111) at incident energies of 80–90 eV in the 45° specular scattering geometry [25]. We consider that the sudden reduction appears as a result of $N_2^+$ dissociation, induced by translational to internal energy transfer. However, this result should be re-examined.

The result obtained in the present study implies that very low energy ion scattering using chemically active ion species is a complementary technique to photoinduced desorption for the study of the chemical interaction potential. The important energy region for this purpose is shown to be 50–100 eV. CO photodesorption has been observed only from Pt surfaces and has not been observed from a less active metal surface (e.g. Cu(111) [26]), in which a longer lifetime is expected in the intermediate excited state of the desorption process. It would therefore be useful to perform very low energy ion scattering experiments for various systems. Further experiments with precise energy analysis of scattered ions are also required in order to discuss the potential energy surface in detail. These studies will open up new avenues in molecule–surface interaction research. We have constructed new apparatus, and are performing experiments including measurement of the angular dependence.

## References


[1] Y. Murata, in: Unimolecular and Bimolecular Reaction Dynamics, Eds. C.Y. Ng, T. Baer and I. Powis (Wiley, Chichester, 1994) p. 427.
[2] H. Akazawa and Y. Murata, Phys. Rev. Lett. 61 (1988) 1218.
[3] H. Akazawa and Y. Murata, Phys. Rev. B 39 (1989) 3449.
[4] A. Peremans, K. Fukutani, K. Mase and Y. Murata, Phys. Rev. B 47 (1993) 4135.
[5] K. Fukutani, M.-B. Song and Y. Murata, J. Chem. Phys. 103 (1995) 2221.
[6] H. Nakatsuji, H. Morita, H. Nakai, Y. Murata and K. Fukutani, J. Chem. Phys. 104 (1996) 714.
[7] H. Akazawa and Y. Murata, J. Chem. Phys. 92 (1990) 5551.
[8] F.I. Dalidchik, S.A. Kovalevskii, N.N. Kolchenko and B.R. Shub, JETP Lett. 58 (1993) 515.
[9] F.I. Dalidchik, M.V. Grishin, S.A. Kovalevskii, N.N. Kolchenko and B.R. Shub, Surf. Sci. 316 (1994) 198.
[10] H. Kaji, K. Makoshi and A. Yoshimori, Surf. Sci. 279 (1992) 165.
[11] K. Fukutani, M.-B. Song and Y. Murata, Faraday Discuss. 96 (1993) 105.
[12] J.A. Prybyla, T.F. Heinz, J.A. Misewich, M.M.T. Loy and J.H. Glownia, Phys. Rev. Lett. 64 (1990) 1537.
[13] H. Nakatsuji and K. Hirao, J. Chem. Phys. 68 (1978) 2035.
[14] H. Nakatsuji, Chem. Phys. Lett. 59 (1978) 362. Chem. Phys. Lett. 67 (1979) 329, 334.
[15] H. Nakatsuji, Chem. Phys. 75 (1983) 425.
[16] H. Nakatsuji, Acta Chim. Hung. 129 (1992) 719.
[17] H.-W. Lee and T.F. George, Surf. Sci. 159 (1985) 214.
[18] R. Hentschke, K.J. Snowdon, P. Hertel and W. Heiland, Surf. Sci. 173 (1986) 565.
[19] H.D. Hagstrum, in: Inelastic Ion–Surface Collisions, Eds. N.H. Tolk, J.C. Tully, W. Heiland and C.W. White (Plenum, New York, 1977) 1.
[20] A.A. Abrahamson, Phys. Rev. 178 (1969) 76.
[21] K. Mase, K. Fukutani and Y. Murata, J. Chem. Phys. 96 (1992) 5523.
[22] M.-B. Song, S. Mizuno, K. Fukutani and Y. Murata, Chem. Phys. Lett. 196 (1992) 559.
[23] A.R. Burns, E.B. Stechel and D.R. Jennison, Phys. Rev. Lett. 58 (1987) 250.
[24] S. Kovalevskii, F. Dalidchik, M. Grishin, N. Kolchenko and B. Shub, Surf. Sci. 331–333 (1995) 317.
[25] M. Okada and Y. Murata, J. Phys.: Condens. Matter 4 (1992) 5097.
[26] J.A. Prybyla, H.W.K. Tom and G.D. Aumiller, Phys. Rev. Lett. 68 (1992) 503.